ChemComm

COMMUNICATION

View Article Online
View Journal | View Issue

Cite this: *Chem. Commun.*, 2015, 51, 10864

Received 12th May 2015,
Accepted 2nd June 2015

DOI: 10.1039/c5cc03934g

www.rsc.org/chemcomm

Effect of the functionalisation route on a Zr-MOF with an Ir–NHC complex for catalysis†

Fabian Carson,[ab] Elisa Martínez-Castro,[ac] Rocío Marcos,[ac] Greco González Miera,[ac] Kjell Jansson,[b] Xiaodong Zou*[ab] and Belén Martín-Matute*[ac]

A new iridium N-heterocyclic carbene (NHC) metallolinker has been synthesised and introduced into a metal–organic framework (MOF), for the first time, *via* two different routes: direct synthesis and postsynthetic exchange (PSE). The two materials were compared in terms of the Ir loading and distribution using X-ray energy dispersive spectroscopy (EDS), the local Ir structure using X-ray absorption spectroscopy (XAS) and the catalytic activity. The materials showed good activity and recyclability as catalysts for the isomerisation of an allylic alcohol.

MOFs are porous coordination networks assembled from metal and organic units.[1] These materials have been investigated for various applications including gas storage and separation, biomedicine and catalysis.[2]

MOFs offer several advantages as supports for transition metal complexes such as high surface areas, tunable and regularly arranged pore environments.[3] There are several routes to introduce linkers containing metal complexes, *i.e.* metallolinkers, into MOFs. The MOF can be directly constructed from the metallolinker.[4] The multivariate (MTV) or mixed-linker approaches allow control of the metallolinker loading in the MOF.[5] Postsynthetic metallation[6] and PSE[7] or solvent-assisted linker exchange have been used to introduce many different metals into MOFs. Although there have been several studies on the spatial distribution of linkers in MTV-MOFs prepared by direct synthesis,[8] there have been few reports concerning the distribution of linkers or metallolinkers in MTV-MOFs prepared by PSE.[7c,9] The distribution of active sites within the MOF will undoubtedly have a direct impact on its catalytic properties.

The σ-electron-donating properties of NHCs as ligands lead to stable metal–NHC complexes,[10] and has resulted in their widespread use as catalysts for numerous transformations, including metathesis reactions, cross-couplings, oxidations and water oxidation.[11] There have been several reports of metal–NHC complexes in MOFs,[12] although the only example of catalysis was a MOF containing Pd–NHC moieties (prepared by metallation of the imidazolium moieties in the MOF) for Suzuki–Miyaura couplings and alkene hydrogenation.[13] Functionalised NHCs with donor groups on the imidazole sidechain can chelate to the metal and improve the catalytic activity.[14] Our group recently reported an alcohol-tethered Ir–NHC complex for hydrogen transfer reactions.[15] The alcohol/alkoxide group participates in the catalytic cycle as a Brønsted acid–base and also forms hydrogen bonds with the reactants.[15b] This bifunctional catalyst is therefore an ideal candidate for immobilisation in a MOF because it avoids the use of base additives that can be detrimental to the MOF structure.[16]

We synthesised a new Ir–NHC metallolinker containing an alcohol donor group, H_2**L** (Fig. 1 and ESI† for full details), and introduced it into a zirconium MOF, UiO-68–2CH_3 (also known as PCN-56),[17] which is constructed from 2′,5′-dimethylterphenyl-4,4″-dicarboxylate (dmtpdc) linkers and Zr clusters. Zr-MOFs are ideal as catalyst supports due to their high thermal and chemical stability.[18] In the first approach, we directly synthesised the MOF from a mixture of H_2dmtpdc and H_2**L** (Fig. 1, direct synthesis). In the second approach, we introduced H_2**L** into UiO-68–2CH_3 through PSE (Fig. 1, postsynthetic exchange). Herein we compare the results between these two approaches in terms of crystallinity, metal loading, porosity, metal distribution and catalytic activity of the MOFs.

The best conditions to synthesise UiO-68–2CH_3 with good crystallinity and a high surface area were with $ZrCl_4$, H_2dmtpdc, H_2O (5 equiv.) and benzoic acid (5 equiv.) in *N*,*N*′-dimethylformamide (DMF) at 70 °C for 72 h.[19] The X-ray powder diffraction (XRPD) pattern of UiO-68–2CH_3 matches with the calculated pattern of UiO-68–2CH_3 (Fig. 2a).[17] LeBail refinement using the XRPD data gave a cubic unit cell, a = 32.902(1) Å, V = 35619(1) Å^3 (Fig. S2, ESI†). Results from elemental analysis and thermogravimetric analysis (TGA) suggested the chemical formula was $[Zr_6O_5(OH)_3(dmtpdc)_{5.5}\cdot 10H_2O]$, with *ca.* one out of 12 linkers missing per zirconium cluster (Fig. S3, ESI†).[20]

[a] *Berzelii Center EXSELENT on Porous Materials, Stockholm University, SE-106 91 Stockholm, Sweden. E-mail: xzou@mmk.su.se, belen.martin.matute@su.se*
[b] *Department of Materials and Environmental Chemistry, Stockholm University, SE-106 91 Stockholm, Sweden*
[c] *Department of Organic Chemistry, Stockholm University, SE-106 91 Stockholm, Sweden*

† Electronic supplementary information (ESI) available: Synthesis, additional characterisation data and catalysis details. See DOI: 10.1039/c5cc03934g

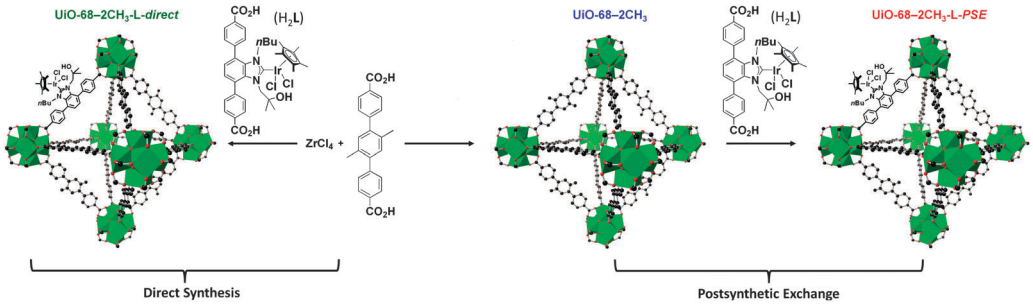

Fig. 1 Schematic representation illustrating the different routes used to introduce the Ir–NHC metallolinker, H_2**L**, into the zirconium MOF.

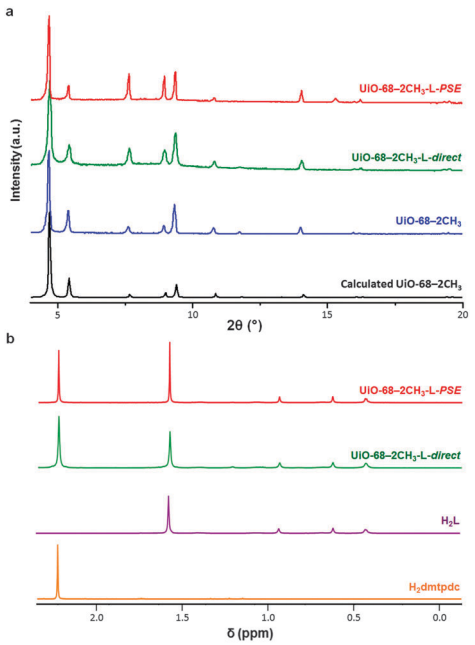

Fig. 2 (a) Calculated (black) and observed XRPD patterns of UiO-68–$2CH_3$ (blue), UiO-68–$2CH_3$-**L**-direct (green) and UiO-68–$2CH_3$-**L**-PSE (red) and (b) ^{1}H NMR spectra of the linkers, H_2dmtpdc and H_2**L**, and the digested MOFs.

For the direct synthesis approach, similar reaction conditions were used with a ratio of H_2dmtpdc : H_2**L** = 60 : 40.

The functionalised MOF was washed with DMF and ethanol and dried under vacuum, yielding a yellow solid referred to as UiO-68–$2CH_3$-**L**-direct. XRPD confirmed the crystallinity of the MOF and the diffraction peaks matched closely with UiO-68–$2CH_3$ (Fig. 2a). The actual ratio of dmtpdc : **L** was determined to be ~83 : 17 by ^{1}H nuclear magnetic resonance (NMR) spectroscopy of the digested MOF (MOF treated in D_3PO_4/d^6-DMSO) (Fig. 2b).[5c] These results, together with those from elemental analysis and TGA, indicated the chemical formula of UiO-68–$2CH_3$-**L**-direct to be $[Zr_6O_5(OH)_3(dmtpdc)_{4.57}\mathbf{L}_{0.94}\cdot 30H_2O]$.

We then tested the PSE route to introduce the metallolinker into the MOF aiming for a ratio of 60 : 40 for dmtpdc : **L**. The best conditions (highest loading of metallolinker while avoiding MOF decomposition) involved heating UiO-68–$2CH_3$ with H_2**L** in methanol at 60 °C for 24 h. After washing with methanol and ethanol and drying under vacuum, a yellow, crystalline solid was recovered, and denoted as UiO-68–$2CH_3$-**L**-PSE (Fig. 2a). The actual ratio of dmtpdc : **L** in UiO-68–$2CH_3$-**L**-PSE was ~71 : 29, which was calculated by ^{1}H NMR spectroscopy (Fig. 2b). This is closer to the intended ratio of 60 : 40 compared to the direct synthesis approach. PSE in DMF gave lower **L** loadings (74 : 26), and in water resulted in MOF decomposition (Fig. S1, ESI†).

Inspection of the IR spectrum of UiO-68–$2CH_3$-**L**-PSE revealed a band at 1687 cm^{-1} that corresponds to the ν(C=O) stretch of the carboxylic acid linkers (Fig. S5, ESI†). In addition, results from elemental analysis indicated additional linker was present. This implies that some linker may not be coordinated to the zirconium clusters in UiO-68–$2CH_3$-**L**-PSE.[21] The chemical formula of UiO-68–$2CH_3$-**L**-PSE was estimated as $[Zr_6O_4(OH)_4(dmtpdc)_{4.62}\mathbf{L}_{1.38}\cdot 0.5H_2\mathbf{L}\cdot 10H_2O]$.[22]

To study the spatial distribution of Ir in the MOFs, we used scanning electron microscopy (SEM) and EDS to measure the element concentrations (Ir and Zr) inside MOF crystals polished with an argon ion-beam. EDS measurements on cross-sections of UiO-68–$2CH_3$-**L**-direct and UiO-68–$2CH_3$-**L**-PSE crystals showed a homogeneous distribution of Ir, which ranged from 0.16–0.24 Ir/Zr in UiO-68–$2CH_3$-**L**-direct and 0.34–0.40 Ir/Zr in UiO-68–$2CH_3$-**L**-PSE (Fig. S8 and S9 and Table S1, ESI†). The metallolinker loadings calculated using different characterisation methods are reported in Table 1. The average Ir loadings estimated by EDS are 19% in UiO-68–$2CH_3$-**L**-direct and 36% in UiO-68–$2CH_3$-**L**-PSE, which are slightly higher than those obtained by inductively coupled plasma optical emission spectrometry (ICP-OES) (14 and 27%, respectively) and ^{1}H NMR analysis of the digested MOFs (17 and 29%, respectively).

We performed Ir L_{III}-edge XAS to confirm the integrity of the Ir complex in the MOF. The X-ray absorption near-edge structure (XANES) spectra of H_2**L**, UiO-68–$2CH_3$-**L**-direct and UiO-68–$2CH_3$-**L**-PSE are similar (Fig. 3), which indicates a similar local coordination environment around Ir. The extended X-ray absorption fine structure (EXAFS) spectra were fitted using crystallographic data from an analogous Ir–NHC complex[12] and the results are displayed

Table 1 Metallolinker loading in MOFs determined using different characterisation methods

Material	^{1}H NMR [%]	ICP-OES [%]	EDS[a] [%]
UiO-68–$2CH_3$-**L**-direct	17	14	19
UiO-68–$2CH_3$-**L**-PSE	29	27	36

[a] Average of eight positions measured on crystal.

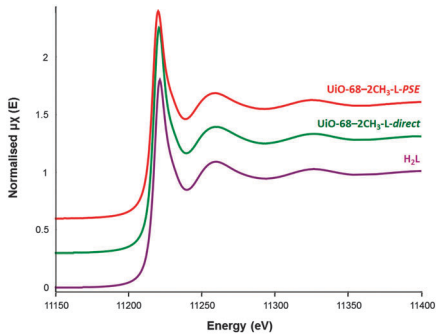

Fig. 3 Ir L_{III}-edge XANES spectra of H_2**L**, UiO-68–2CH_3-**L**-direct and UiO-68–2CH_3-**L**-PSE.

in Table S2, ESI.† The first and second shells around iridium were included in the fit and similar distances were attained in H_2**L**, UiO-68–2CH_3-**L**-direct and UiO-68–2CH_3-**L**-PSE, confirming the structure of the Ir–NHC complex in the MOFs.

UiO-68–2CH_3 was thermally stable up to 400 °C in air according to TGA measurements (Fig. S3, ESI†). Both UiO-68–2CH_3-**L**-direct and UiO-68–2CH_3-**L**-PSE were less stable than UiO-68–2CH_3 and displayed weight losses at 200 °C, probably corresponding to decomposition of the Ir–NHC complex. The porosity of the MOFs was studied by N_2 adsorption (Fig. S14, ESI†). The BET surface area of the MOFs progressively decreased with increasing metallolinker loading, from 2470 $m^2\ g^{-1}$ for UiO-68–2CH_3 to 2040 and 1600 $m^2\ g^{-1}$ for UiO-68–2CH_3-**L**-direct and UiO-68–2CH_3-**L**-PSE, respectively (Table S3, ESI†).

We then compared the performance of these materials as catalysts for the isomerisation of a model allylic alcohol substrate, 1-octen-3-ol.[22] There have been no reports of MOFs as catalysts for the isomerisation of allylic alcohols, although other materials, such as Ru and Rh complexes supported on alumina and mesoporous silica, respectively, have been used to isomerise allylic alcohols.[23]

We compared the catalytic activity of the ester-protected Ir–NHC metallolinker **9** (see Section S6, ESI†), UiO-68–2CH_3-**L**-direct and UiO-68–2CH_3-**L**-PSE for the isomerisation of 1-octen-3-ol at 100 °C in toluene using 4 mol% Ir. The blank reactions (with no catalyst or with UiO-68–2CH_3) gave 0% yield after 24 h (Table 2, entries 1 and 2). The metallolinker reached >99% yield of 3-octanone after 24 h in the absence of any additive (Table 2, entry 3). UiO-68–2CH_3-**L**-direct and UiO-68–2CH_3-**L**-PSE showed similar catalytic activity, achieving 64% and 65% yield, respectively, after 48 h (Table 2, entries 4 and 5). XRPD analysis of the MOFs after catalysis showed they retained their crystallinity (Fig. S15, ESI†). ICP-OES analysis revealed that less than 1 ppm Ir was present in the supernatant after catalysis with UiO-68–2CH_3-**L**-PSE, which indicates that the metallolinker did not leach out of the material during catalysis. On the other hand, the Ir content in the supernatant after catalysis was higher (7.5 ppm) for UiO-68–2CH_3-**L**-direct. Therefore, we pursued further catalytic tests with only UiO-68–2CH_3-**L**-PSE. The catalytic activity of UiO-68–2CH_3-**L**-PSE was improved by adding $AgBF_4$ (10 mol%).[12] This resulted in 80% yield after 24 h (Table 2, entry 6), although the Ir leaching increased slightly (1.7 ppm Ir was detected in the supernatant) and the MOF after catalysis was less crystalline (Fig. S12, ESI†). Replacing $AgBF_4$ for bases, such as $NaHCO_3$ and K_2CO_3, resulted in 99% yield after

Table 2 Comparison of different catalysts for isomerisation of 1-octen-3-ol[a]

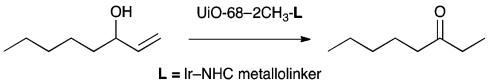

Entry	Catalyst	Additive	t [h]	Yield[b] [%]
1	Blank	—	24	0
2	UiO-68–2CH_3	—	24	0
3	**9** (metallolinker)	—	24	>99
4	UiO-68–2CH_3-**L**-direct	—	48	64
5	UiO-68–2CH_3-**L**-PSE	—	48	65
6	UiO-68–2CH_3-**L**-PSE	$AgBF_4$[c]	24	80
7	UiO-68–2CH_3-**L**-PSE	$NaHCO_3$[d]	24	>99
8	UiO-68–2CH_3-**L**-PSE	K_2CO_3[d]	24	>99

[a] Reagents and conditions: 1-octen-3-ol (0.1 mmol, 14 μL) and catalyst (4 mol% Ir) were suspended in toluene (1 mL) and stirred vigorously at 100 °C for 24 or 48 h. [b] Yield of 3-octanone based on ^{1}H NMR spectroscopy of the crude reaction mixture. [c] The MOF was stirred with $AgBF_4$ (0.01 mmol, 10 mol%) in toluene prior to the addition of the alcohol. [d] 1 equiv. was used.

24 h (Table 2, entries 7 and 8); however, the Ir leaching was significantly higher (32 and 5.8 ppm for $NaHCO_3$ and K_2CO_3, respectively) and the crystallinity of the recovered MOF was affected (Fig. S12, ESI†). This agrees with our previous findings on the effect of the base on the MOF's structure,[16] and demonstrates the advantage of immobilising bifunctional catalysts. On a larger scale experiment and under otherwise identical conditions as those used in Table 2, entry 5, UiO-68–2CH_3-**L**-PSE afforded 99% conversion in the absence of base and could be recycled three times without any loss in catalytic activity (Table S5, ESI†).[24] The heterogeneity of the catalyst was studied by filtering the catalyst after 3 h, with no further increase in the yield after 18 h.

These results demonstrate the importance of the different functionalisation routes for introducing metal complexes into MOFs and the effect on the properties and catalytic performance of the material. PSE is a powerful approach for introducing metallolinkers into MOFs which, in this case, can lead to higher metal loadings compared to direct synthesis. The combination of characterisation methods used here, in particular XAS and EDS, has enabled the structure and distribution of the metal complex inside the MOF crystals to be studied. By using a robust zirconium MOF as the support, together with a highly stable bifunctional Ir–NHC complex, a porous, recyclable heterogeneous catalyst has been prepared, which demonstrates that UiO-68 is an ideal MOF for creating advanced catalytic materials.

This work was supported by the Swedish Research Council (VR) and the Swedish Governmental Agency for Innovation Systems (VINNOVA) through the Berzelii Center EXSELENT, Röntgen-Ångström Cluster through VR (MATsynCELL), and the Knut and Alice Wallenberg Foundation (Catalysis in Selective Organic Synthesis and 3DEM-NATUR). BMM was supported by VINNOVA through a VINNMER fellowship. EMC and RM thank the Wenner-Gren foundation for post-doctoral fellowships. Portions of this research were conducted at beamline I811 (MAX IV Laboratory, Lund, Sweden). We thank Lara Schultes for the synthesis of organic linkers and Ingmar Persson, Ning Yuan and Stefan Carlson for their assistance with XAS measurements and interpretations.

Notes and references

1 S. R. Batten, N. R. Champness, X.-M. Chen, J. Garcia-Martinez, S. Kitagawa, L. Öhrström, M. O'Keeffe, M. Paik Suh and J. Reedijk, *Pure Appl. Chem.*, 2013, **85**, 1715–1724.

2 (*a*) K. Sumida, D. L. Rogow, J. A. Mason, T. M. McDonald, E. D. Bloch, Z. R. Herm, T.-H. Bae and J. R. Long, *Chem. Rev.*, 2012, **112**, 724–781; (*b*) P. Horcajada, R. Gref, T. Baati, P. K. Allan, G. Maurin, P. Couvreur, G. Férey, R. E. Morris and C. Serre, *Chem. Rev.*, 2012, **112**, 1232–1268; (*c*) J. Liu, L. Chen, H. Cui, J. Zhang, L. Zhang and C.-Y. Su, *Chem. Soc. Rev.*, 2014, **43**, 6011–6061.

3 (*a*) G. Férey, *Chem. Soc. Rev.*, 2008, **37**, 191–214; (*b*) W. Lu, Z. Wei, Z.-Y. Gu, T.-F. Liu, J. Park, J. Park, J. Tian, M. Zhang, Q. Zhang, T. Gentle III, M. Bosch and H.-C. Zhou, *Chem. Soc. Rev.*, 2014, **43**, 5561–5593.

4 (*a*) C. A. Kent, B. P. Mehl, L. Ma, J. M. Papanikolas, T. J. Meyer and W. Lin, *J. Am. Chem. Soc.*, 2010, **132**, 12767–12769; (*b*) F. Song, C. Wang, J. M. Falkowski, L. Ma and W. Lin, *J. Am. Chem. Soc.*, 2010, **132**, 15390–15398.

5 (*a*) H. Deng, C. J. Doonan, H. Furukawa, R. B. Ferreira, J. Towne, C. B. Knobler, B. Wang and O. M. Yaghi, *Science*, 2010, **327**, 846–850; (*b*) C. Wang, Z. Xie, K. E. deKrafft and W. Lin, *J. Am. Chem. Soc.*, 2011, **133**, 13445–13454; (*c*) A. E. Platero-Prats, A. Bermejo Gómez, L. Samain, X. Zou and B. Martín-Matute, *Chem. – Eur. J.*, 2015, **21**, 861–866.

6 (*a*) E. D. Bloch, D. Britt, C. Lee, C. J. Doonan, F. J. Uribe-Romo, H. Furukawa, J. R. Long and O. M. Yaghi, *J. Am. Chem. Soc.*, 2010, **132**, 14382–14384; (*b*) F. Carson, S. Agrawal, M. Gustafsson, A. Bartoszewicz, F. Moraga, X. Zou and B. Martín-Matute, *Chem. – Eur. J.*, 2012, **18**, 15337–15344; (*c*) M. Pintado-Sierra, A. M. Rasero-Almansa, A. Corma, M. Iglesias and F. Sánchez, *J. Catal.*, 2013, **299**, 137–145; (*d*) H. Fei and S. M. Cohen, *Chem. Commun.*, 2014, **50**, 4810–4812.

7 (*a*) C. Y. Lee, O. K. Farha, B. J. Hong, A. A. Sarjeant, S. T. Nguyen and J. T. Hupp, *J. Am. Chem. Soc.*, 2011, **133**, 15858–15861; (*b*) M. Kim, J. F. Cahill, H. Fei, K. A. Prather and S. M. Cohen, *J. Am. Chem. Soc.*, 2012, **134**, 18082–18088; (*c*) S. Takaishi, E. J. DeMarco, M. J. Pellin, O. K. Farha and J. T. Hupp, *Chem. Sci.*, 2013, **4**, 1509–1513; (*d*) S. Pullen, H. Fei, A. Orthaber, S. M. Cohen and S. Ott, *J. Am. Chem. Soc.*, 2013, **135**, 16997–17003.

8 (*a*) S. Furukawa, K. Hirai, Y. Takashima, K. Nakagawa, M. Kondo, T. Tsuruoka, O. Sakata and S. Kitagawa, *Chem. Commun.*, 2009, 5097–5099; (*b*) X. Kong, H. Deng, F. Yan, J. Kim, J. A. Swisher, B. Smit, O. M. Yaghi and J. A. Reimer, *Science*, 2013, **341**, 882–885.

9 A. M. Katzenmeyer, J. Canivet, G. Holland, D. Farrusseng and A. Centrone, *Angew. Chem., Int. Ed.*, 2014, **53**, 2852–2856.

10 (*a*) W. A. Herrmann and C. Köcher, *Angew. Chem., Int. Ed.*, 1997, **36**, 2162–2187; (*b*) C. M. Crudden and D. P. Allen, *Coord. Chem. Rev.*, 2004, **248**, 2247–2273.

11 (*a*) M. N. Hopkinson, C. Richter, M. Schedler and F. Glorius, *Nature*, 2014, **510**, 485–496; (*b*) G. C. Vougioukalakis and R. H. Grubbs, *Chem. Rev.*, 2010, **110**, 1746–1787; (*c*) E. A. B. Kantchev, C. J. O'Brien and M. G. Organ, *Angew. Chem., Int. Ed.*, 2007, **46**, 2768–2813; (*d*) D. R. Jensen, M. J. Schultz, J. A. Mueller and M. S. Sigman, *Angew. Chem., Int. Ed.*, 2003, **42**, 3810–3813; (*e*) I. Corbucci, A. Petronilho, H. Müller-Bunz, L. Rocchigiani, M. Albrecht and A. Macchioni, *ACS Catal.*, 2015, **5**, 2714–2718.

12 (*a*) J. Chun, I. G. Jung, H. J. Kim, M. Park, M. S. Lah and S. U. Son, *Inorg. Chem.*, 2009, **48**, 6353–6355; (*b*) J. Chun, H. S. Lee, I. G. Jung, S. W. Lee, H. J. Kim and S. U. Son, *Organometallics*, 2010, **29**, 1518–1521; (*c*) K. Oisaki, Q. Li, H. Furukawa, A. U. Czaja and O. M. Yaghi, *J. Am. Chem. Soc.*, 2010, **132**, 9262–9264.

13 (*a*) G.-Q. Kong, X. Xu, C. Zou and C.-D. Wu, *Chem. Commun.*, 2011, **47**, 11005–11007; (*b*) G.-Q. Kong, S. Ou, C. Zou and C.-D. Wu, *J. Am. Chem. Soc.*, 2012, **134**, 19851–19857.

14 S. T. Liddle, I. S. Edworthy and P. L. Arnold, *Chem. Soc. Rev.*, 2007, **36**, 1732–1744.

15 (*a*) A. Bartoszewicz, R. Marcos, S. Sahoo, A. K. Inge, X. Zou and B. Martín-Matute, *Chem. – Eur. J.*, 2012, **18**, 14510–14519; (*b*) A. Bartoszewicz, G. González Miera, R. Marcos, P.-O. Norrby and B. Martín-Matute, *ACS Catal.*, 2015, **5**, 3704–3716.

16 F. Carson, V. Pascanu, A. Bermejo Gómez, Y. Zhang, A. E. Platero-Prats, X. Zou and B. Martín-Matute, *Chem. – Eur. J.*, 2015, DOI: 10.1002/chem.201500843.

17 H.-L. Jiang, D. Feng, T.-F. Liu, J.-R. Li and H.-C. Zhou, *J. Am. Chem. Soc.*, 2012, **134**, 14690–14693.

18 (*a*) J. H. Cavka, S. Jakobsen, U. Olsbye, N. Guillou, C. Lamberti, S. Bordiga and K. P. Lillerud, *J. Am. Chem. Soc.*, 2008, **130**, 13850–13851.

19 We were unable to synthesise crystalline UiO-68 with terphenyldicarboxylic acid (tpdc) using similar synthesis conditions. This may be due to the poorer solubility of tpdc compared to dmtpdc.

20 (*a*) H. Wu, Y. S. Chua, V. Krungleviciute, M. Tyagi, P. Chen, T. Yildirim and W. Zhou, *J. Am. Chem. Soc.*, 2013, **135**, 10525–10532; (*b*) F. Vermoortele, B. Bueken, G. Le Bars, B. Van de Voorde, M. Vandichel, K. Houthoofd, A. Vimont, M. Daturi, M. Waroquier, V. Van Speybroeck, C. Kirschhock and D. E. De Vos, *J. Am. Chem. Soc.*, 2013, **135**, 11465–11468; (*c*) S. Øien, D. Wragg, H. Reinsch, S. Svelle, S. Bordiga, C. Lamberti and K. P. Lillerud, *Cryst. Growth Des.*, 2014, **14**, 5370–5372.

21 Alternatively, the metallolinker may only be coordinated to zirconium at one side and protonated at the other side. In addition, ^{1}H NMR analysis of the supernatant after PSE revealed the presence of H_2dmtpdc, which indicates that exchange of the linkers occurred.

22 (*a*) N. Ahlsten, A. Bartoszewicz and B. Martín-Matute, *Dalton Trans.*, 2012, **41**, 1660–1670; (*b*) N. Ahlsten, A. Bermejo Gómez and B. Martín-Matute, *Angew. Chem., Int. Ed.*, 2013, **52**, 6273–6276.

23 (*a*) K. Yamaguchi, T. Koike, M. Kotani, M. Matsushita, S. Shinachi and N. Mizuno, *Chem. – Eur. J.*, 2005, **11**, 6574–6582; (*b*) S. Sahoo, H. Lundberg, M. Edén, N. Ahlsten, W. Wan, X. Zou and B. Martín-Matute, *ChemCatChem*, 2012, **4**, 243–250.

24 The larger scale reaction was carried out using 0.38 mmol of substrate instead of 0.10 mmol. The higher yield may be due to better mixing of the reaction mixture on a larger scale.